Hindawi
Journal of Chemistry
Volume 2022, Article ID 4849758, 13 pages
https://doi.org/10.1155/2022/4849758

Research Article

Adsorptive Removal of Methylene Blue Dye Using Biowaste Materials: Barley Bran and Enset Midrib Leaf

Dereje Mekuria[1], **Abebe Diro**[1], **Fekadu Melak**[1,2] and **Tsegaye Girma Asere**[1]

[1]*Department of Chemistry, College of Natural Sciences, Jimma University, P.O. Box 378, Jimma, Ethiopia*
[2]*Department of Environmental Health, College of Health Sciences, Debre Markos University, Ethiopia*

Correspondence should be addressed to Tsegaye Girma Asere; tsegaye96@gmail.com

Received 15 February 2022; Accepted 12 April 2022; Published 28 April 2022

Academic Editor: Rabia Rehman

In this study, several biowaste materials are screened for adsorptive removal of methylene blue (MB) from synthetic water. Among the tested adsorbents, barley (*Hordeum vulgare*) bran (BB) and enset (*Ensete ventricosum* midrib leaf, EVML) were selected for further evaluation of MB (a model cationic dye) adsorption. Batch MB adsorption performance of BB and EVML adsorbents was significantly high in a wide pH range (4-9). The well fitting of experimental data with pseudosecond-order kinetic model suggests a monolayer adsorption of MB. The MB adsorption onto both adsorbents was fit well with the Langmuir isotherm model with maximum MB adsorption capacities of 63.2 mg/g (BB) and 35.5 mg/g (EVML). The biowaste materials exhibit considerable adsorption capacity for cationic dye (MB), perform well under acidic and basic conditions, and are reusable. Therefore, the use of these materials as adsorbents may have an environmental benefit in terms of the conversion of wastes into valuable materials. Further studies are suggested to investigate the performance of these adsorbents in a continuous mode using real wastewater.

1. Introduction

Discharging industrial effluents directly into water bodies without proper treatment can create water pollution [1]. For instance, textile manufacturing uses various types of dyes, chemicals, and large volumes of water in fabric production. Direct release of this dye-contaminated water into the environment can affect human health, soil, and aquatic life [2]. Dye effluents are among those contaminants that have caused significant water pollution worldwide [3]. Dyes are substances obtained either naturally from extracts of flowers, fruits, certain insects, etc. or from synthetic sources that give colors [4]. Natural dyes have inherent weaknesses such as offering a narrow range of colors, low fastness to fabrics, fade on washing, and exposure to light [5]. On the other hand, synthetic dyes provide several colorfast dyes in a wide color range, which led to their mass industrial production [4]. The wide production of various synthetic dyes leads to the discharge of a considerable volume of dye-contaminated wastewater into the environment, which becomes one of the causes of water contamination [6].

Generally, synthetic dyes have low biodegradability due to the presence of complex aromatic molecular structures [2]. They are water-soluble and produce very bright colors in the water, particularly those dyes used in textile industries. Textile manufacturing consumes greater than 1000 tons of dyes per annum, where about 10-15% of them are directly discharged into the water bodies through the sewerage system [7]. These effluents contain a mixture of different dyes, auxiliaries, additives, and additional chemicals that may disturb the aquatic system. Small amounts of dyes in water (as low as 1.0 ppm) could bring substantial color, making it unsuitable for human usage [8]. Dyes can also reduce the light transmission and thus diminish the photosynthetic processes of water bodies and imbalance the aquatic system [9, 10]. The problems become serious due to them are stable in different situations such as heat, light, microbes, and even oxidizing agents [11]. Hence, the removal of dyes from

water/wastewater by using different technologies is still an ongoing research topic.

Many treatment methods have been used for removing dyes from waterwater. The typical treatment methods comprise ion exchange, membrane system (reverse osmosis, electroflotation, nanofiltration), adsorption, coagulation/flocculation, advanced oxidation, ozonation, electrokinetic coagulation, microbial degradation, electrochemical destruction, and precipitation [9, 12, 13]. Adsorption is the commonly utilized treatment technology owing to its flexibility, user friendly, economical, nice performance, recyclability, and being ecofriendly [14]. The common adsorbent, a commercial activated carbon, is costly to use in real applications in different regions of the globe, particularly in developing nations. This has motivated researchers for exploring low-cost, efficient, high carbon content, and renewable adsorbents, which has led to increasing attention in the usage of locally accessible resources, for example, natural materials and agricultural debris [15]. Therefore, this study was intended to evaluate the methylene blue (MB, model dye) adsorption efficiency of selected biowastes accessible in Ethiopia: the petiole of enset (*Ensete ventricosum*) and barley bran (*Hordeum vulgare* L. (Poaceae).

2. Materials and Methods

2.1. Chemicals and Apparatuses. A stock solution of 1000 mg/L MB was prepared, wrap with aluminum foil, and put in a cabinet to protect it from light interaction. Standard and working solutions were prepared by diluting the stock solution. The pH of working solutions was adjusted using 0.1 M HCl (37%, Riedel-deHaën, Germany) and 0.1 M NaOH (90%, BDH, England) solutions. Distilled water was used to prepare and dilute the stock solution. Freshly prepared different concentrations of MB were immediately utilized for the desired experiments. Horizontal GFL shaker (memmert, D-30938, Germany) for the batch adsorption, digital pH meter ORION star A211 for pH measurement, respectively.

2.2. Preparation of Biowaste Materials. Biowaste materials such as avocado (*Persea americana*) seed (AS), enset (*Ensete ventricosum)* midrib leaf (EVML), barley (*Hordeum vulgare* L. (Poaceae) bran (BB), coffee (*Coffea arabica* L) residue (CR), "Tella" residue (TR), eucalyptus tree ash (ETA), acacia tree charcoal (ATC), pea (*Pisum sativum*) seed shell (PSS), and *Erythrina abyssinica* bark (EAB) locally called "Korch" were obtained from various locations of Jimma city, Ethiopia. "Tella" residue (TR) and the pea (*Pisum sativum*) seed shell (PSS) were treated as in literature [16]. Both AS and CR were obtained from local cafeterias, whereas BB, TR, ETA, ATC, and PSS were collected from local household wastes. "Korch" is a wild plant that is also cultivated in different regions of Ethiopia and used to make fences around houses and farmlands in rural areas. Enset belongs to the banana family Musaceae, which is widely domesticated in Ethiopia. It is the primary source of food for many people living in the South and Southwest Ethiopia. The root and stem parts of enset are used as food, whereas the leaves are used to wrap cheese, butter, etc. However, the midrib of the leaf is usually a local waste material. "Tella" is one of the traditionally fermented beverages that is regularly prepared and drunk in Ethiopia. Barley, maize, wheat, hops, and other spices are among the commonly used raw materials in the preparation of "Tella." Preparation of "Tella" requires 5–7 days, wherein the final stage, the potable "Tell" is filtered to remove any suspended solid while the settled residue is used to feed cows or discard [16].

All the collected adsorbents were cleaned and rinsed with distilled water before chopped (in the case of AS, EAB, and EVML) and then dried in air. Mortar and pestle were used to ground the adsorbents, then sieved to the mesh size $\leq 300\,\mu$m, and kept in closed vessels until further use. In the case of EVML, 50 g of the adsorbent (size of $\leq 300\,\mu$m) was added to 250 mL of 0.1 M HCl containing flask and shaken for 6 h to remove colored components. Then, the adsorbent was thoroughly washed with distilled water to get rid of the excess acid and allowed to dry in an oven at 80°C.

2.3. Characterization of Adsorbents

2.3.1. Physicochemical Characteristics. The pH and point of zero charges (pHpzc) of BB and EVML adsorbents were evaluated following the procedures used in [17, 18]. The surface area of the biomaterials was estimated following Sear's method [19]. Moisture and ash contents of the adsorbents were calculated following the common procedures ASTM D2867-91 method [20] and ASTM D2866-94 [21], respectively.

2.3.2. FTIR Spectral Analysis. The BB and EVML adsorbents (before and after adsorption of MB) were characterized using Fourier transform infrared (FTIR) to locate functional groups that might participate in the MB adsorption. KBr pellet of each adsorbent of an appropriate thickness for infrared analysis was prepared. FTIR spectrophotometer (Perkin Elmer Spectrum 2.0) in a wavenumber range of 400 to 4000 cm^{-1} was used.

2.4. Batch Adsorption Study. Preliminary screening investigations were done to select biowastes (adsorbents) with high MB adsorption capacity at fixed equilibrium experimental conditions. For this purpose, nine (9) different biowaste materials, namely, avocado (*Persea americana*) seed (AS), *Ensete ventricosum* midrib leaf (EVML), barley (*Hordeum vulgare* L. (Poaceae) bran (BB), coffee (*Coffea arabica* L) residue (CR), "Tella" residue (TR), eucalyptus tree ash (ETA), acacia tree charcoal (ATC), pea (*Pisum sativum*) seed shell (PSS), and *Erythrina abyssinica* bark (EAB) were tested for MB adsorption from contaminated water. The adsorbents were tested under similar settings: 10 mg/L of MB solution, 2.5 g/L of adsorbent dose, and pH 5.7. The batch adsorptions were conducted at room temperature agitated on a horizontal thermostat water bath shaker (GrantGLS400, England) for 24 h at a speed of 200 rpm. Then, it was centrifuged and filtered, and the concentration (mg/L) of the residual MB in the filtrate was measured at λ_{max} (665 nm) after each calibration curve using a double beam UV-VIS spectrophotometer (Analytic Jena Specord200 Plus, Germany). The MB

removal effectiveness (%) and the MB adsorption capacity (mg/g) were evaluated using Eqs. (1) and (2), respectively.

$$\text{MB removal}\,(\%) = \left(\frac{C_0 - C_e}{C_0}\right) \times 100 \quad (1)$$

$$q_e = (C_0 - C_e)\frac{V}{m} \quad (2)$$

where C_0 and C_e are the initial and equilibrium concentration of MB solution (mg/L), respectively, m is the mass (g) adsorbent and V is the volume of solution (L).

Subsequently, the adsorption behaviors of BB and EVML toward anionic dyes (methyl orange (MO), Erichrome black T (EBT)), and cationic dyes (malachite green (MG), brilliant green (BG) were studied in addition to MB. This study was also performed for each dye using 10 mg/L of initial concentration without pH adjustment, an adsorbent dose of 2.5 g/L, and a contact time of 24 h. All experiments were done in duplicate, and the obtained results were reported as mean ± standard deviation.

2.5. Data Analysis

2.5.1. Adsorption Kinetics. To examine the effect of contact time, batch adsorption studies were performed employing 10 mg/L MB in polyethylene containers at the dose of 2.5 g/L BB and EVML and shaking in a water bath at 200 rpm from 5 min to 24 h and 1 min to 2 h, respectively. Samples were collected at predetermined distinct contact times. Then, it was centrifuged and filtered, and the residual-MB concentration of the filtrate was measured at λ_{max} (665 nm). Pseudofirst-order (PFO) and pseudosecond-order (PSO) adsorption kinetic models were employed to evaluate the kinetics of MB adsorption onto BB and EVML adsorbents. The nonlinear expressions of the PFO and PSO models are given in Eqs. (3) and (4), respectively.

$$q_t = q_e\left(1 - \exp^{-K_1 t}\right) \quad (3)$$

$$q_t = \frac{K_2 q_e^2 t}{1 + K_2 q_e t} \quad (4)$$

where q_t and q_e are the MB adsorption capacity (mg/g) at any time and at equilibrium, respectively, and k_1 and k_2 are the PFO (L/min) and PSO (g/mg min) rate constants, respectively.

To predict the potential rate-limiting steps in the adsorption progressions, intraparticle diffusion was evaluated using the Weber Morris model as presented in Eq. (5) [22]. Pore or internal diffusion was stipulated by employing the relationship between specific sorption (q_t) and time ($t^{0.5}$) in the model.

$$q_t = k_p t^{0.5} + c \quad (5)$$

where q_t is the amount of MB adsorbed on BB or EVML (mg/g) at time t, k_p (mg/(g.min$^{0.5}$) is the intraparticle diffusion rate constant; if the plot of q_t against $t^{1/2}$ is a linear and pass through the origin, it suggests that intraparticle diffusion is the rate-limiting step of MB adsorption.

2.5.2. Adsorption Isotherms. Adsorption isotherms were determined at 24 ± 1°C by employing BB and EVML adsorbents. Constant adsorbent dosage (2.5 g/L) was added to a series of increasing MB concentrations from 10 to 165 mg/L and 10 to 105 mg/L for BB and EVML adsorbents, respectively. The mixtures were agitated until the equilibrium time, and the remaining MB in the filtrate was measured after centrifuging it. The equilibrium experimental data of MB adsorption onto BB and EVML were studied using Langmuir and Freundlich models. The Langmuir isotherm is a monolayer adsorption phenomenon, whereas the Freundlich isotherm model assumes multilayer adsorption. The nonlinear forms of the Langmuir and Freundlich isotherm models are as given in Eqs. (6) and (7), respectively [17].

$$q_e = \frac{Q_{max} b C_e}{(1 + bC_e)} \quad (6)$$

$$q_e = K_F C_e^{1/n} \quad (7)$$

where C_e (mg/L) is the equilibrium concentration of MB, Q_{max} (mg/g) is the maximum adsorption capacity based on the Langmuir equation, b (L/mg) is the Langmuir constant, K_F (mg$^{1-1/n}$ L$^{1/n}$/g) is the sorption coefficient based on the Freundlich equation, and $^1/n$ is the sorption intensity based on the Freundlich equation.

2.5.3. Statistical Test. In addition to the correlation coefficient (R^2), the nonlinear chi-square (χ^2) statistic test was employed to distinguish the best model fit to the obtained experimental data. A small χ^2 value shows the similarity of data between the modeled and the experimental data, whereas a greater χ^2 means variation within the modeled and experimental data. The χ^2 is computed using Eq. (8) [17].

$$\chi^2 = \sum \frac{(q_e - q_{e,cal})^2}{q_{e,cal}} \quad (8)$$

where $q_{e,cal}$ is the equilibrium adsorption capacity computed from the model, and q_e is the experimental equilibrium adsorption capacity.

2.6. Adsorption Cycle. Reusability of BB and EVML adsorbents was tested by keeping the optimum adsorption operating conditions like contact time, adsorbent dose, pH of MB solution, and initial concentration of MB (10 mg/L) dye. The adsorption cycles were determined without desorbing the previously 10 mg/L MB-loaded adsorbents. The experiments were done by carefully decanting the supernatant residual MB solution and then allowing the MB-loaded adsorbents to dry to open air before the 2nd cycle MB adsorption test and so on.

3. Results and Discussion

3.1. Characterization of Adsorbents. Determining the physicochemical properties and/or nature of adsorbents is basic to understanding the adsorption efficiency or capacity of the adsorbents. Hereby, the major physicochemical properties of BB and EVML are illustrated in Table 1. Adsorbent features, including low moisture content and high value of dry matter, are important for the adsorption processes.

The FTIR of BB and EVML was analyzed, and the obtained spectral data is shown in Figure 1. Several bands with different intensity were observed in the spectra region of 4000 cm^{-1} to 500 cm^{-1}. Figure 1(a) displays the FTIR results of BB before and after MB adsorption, whereas Figure 1(b) gives the spectra of EVML before and after MB adsorption. The observed change in intensity of absorption bands and/or a shift in frequency after MB adsorption may indicate the interaction of MB with the functional groups available on the surfaces the BB and EVML [23].

The band near 3428 cm^{-1} in the FTIR of BB shows the existence of –OH groups in BB (Figure 1(a)). The bands in the region 2922 cm^{-1} and 2852 cm^{-1} could be due to the asymmetrical and symmetrical stretching vibrations of the CH_2 group with a saturated carbon [24]. The peak around 1640 cm^{-1} may either be ascribed to C=C stretching of alkene or N–H bending of amine [23]. The weak bands around 1383 cm^{-1} and 1418 cm^{-1} could be due to -CH_2 bending. The band at 1040 cm^{-1} was assigned to be the C–O and COO– stretching, indicating the presence of carboxylic groups in BB Figure 1(a) [25]. From the FTIR spectrum of EVML (Figure 1(b)), the band at 3410 cm^{-1} is because of the O-H (hydroxyl) group stretching vibration, seemingly N-H medium peak overlapping near to 3480 cm^{-1}. The band near 2920 cm^{-1} indicates the notable C-H stretching in the lignin functionality as explained in the literature [26]. The band around 1620 cm^{-1} is ascribed to the C=O (carbonyl) group stretching. The weak band near 1316 may be due to C-N bending in the amino group. The adsorption band observed around 1055 cm^{-1} matches the C–O stretching [27].

3.2. Screening of Biowaste Materials. The MB removal efficiencies of nine locally available biowaste materials were under similar conditions, and the obtained results are demonstrated in Figure 2. The MB adsorption efficiency of BB, EAB, CR, and EVML was ≥95%. The PSS and TR showed similar MB removal efficiency (~90%) under the specified conditions. However, if any of these conditions (initial MB concentration, pH, etc.) change, the two adsorbents may not have similar MB removal potential.

Among the considered adsorbents, BB and EVML were selected because of their high MB removal efficiency. To the best of our knowledge, there was no previous report on these biowastes as adsorbents. The selected adsorbents (BB and EVML) were also evaluated for their anionic dyes methyl orange (MO) and Erichrome Black T (EBT) and cationic dyes malachite green (MG) and brilliant green (BG) removal efficiency at two different concentrations (10 mg/L and 20 mg/L) in their natural (nonadjusted) pH 5.62 and 5.68, 5.59 and 5.53, 4.82 and 4.55, and 4.99 and 4.26, respectively. Figure 3 shows the obtained results.

Table 1: Physiochemical properties of BB and EVML adsorbents.

Parameter	BB	EVML
Moisture content %	3.0	4.0
Dry matter %	97.0	96.0
Ash %	10.2	8.8
Surface area (m^2/g)	26.2	20.34
pH in water	6.47	4.53
pH_{PZC}	5.9	3.5

Both adsorbents effectively removed the cationic dyes MB, BG, and MG compared to the anionic dyes MO and EBT. It may be due to the surface of the adsorbents being negatively charged under the above-specified pH since the pH of zero charge of adsorbents, BB, and EVML was found to be 5.9 and 3.5, respectively. The negatively charged surface of the adsorbents imparts electrostatic interactions to bind cationic dyes (MB, BG, and MG) while repelling the anionic dyes MO and EBT). The negative charge on the anionic dyes is due to the functional group SO_3^-. Note that the SO_3H group having a pKa of -2.1 is expected to be dissociated to SO_3^- even at pH 2 [28]. Therefore, the adsorption properties of BB and EVML were further studied using MB as a model cationic dye.

3.3. Effect of Agitation Time. The influence of agitation time on the removal of MB was evaluated for the agitation time of 5 min to 24 h and 1 min to 2 h for BB and EVML adsorbents, respectively. The obtained results were presented in Figure 4(a) and 4(b). As the contact time increases, the MB adsorption onto both adsorbents increases. Rapid adsorption at the beginning was observed until 20 min and 2 h for EVML and BB, respectively. Afterward, only a gradual increment was observed for both adsorbents because of attaining adsorption equilibrium. That is, the MB adsorption and desorption proceeded nearly at equal rates. However, to ensure maximum MB adsorption and avoid uncertainties in the equilibrium, 4 h was considered for BB, whereas 1 h for EVML for the subsequent adsorption analysis and other adsorption parameter optimizations.

3.4. Kinetics. Kinetics governing the adsorption procedure is among the critical factors that must be considered in designing an adsorption system. The time-dependent MB adsorption onto BB and EVML was estimated by fitting the laboratory obtained results into the nonlinear form of pseudofirst-order (PFO) and pseudosecond-order (PSO) models (Eqs. (3) and (4)). The obtained information from the fitting models is shown in Figures 5(a) and 5(b). The better-fitted model was identified by comparing their correlation coefficient (R^2) and the nonlinear chi-square (χ^2) values (Table 2). Table 2 indicates that the kinetics of obtained experimental data for both adsorbents can be described by using the PSO model rather than the PFO. Besides, the experimental q_e values matched with the calculated q_e values found

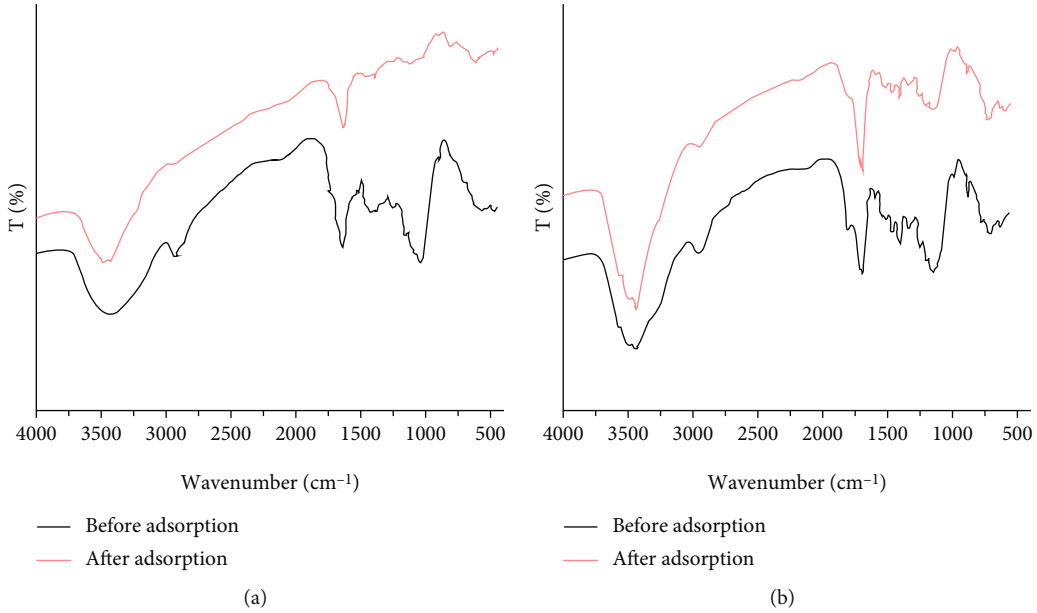

Figure 1: FTIR spectra of (a) BB and (b) EVML before and after adsorption.

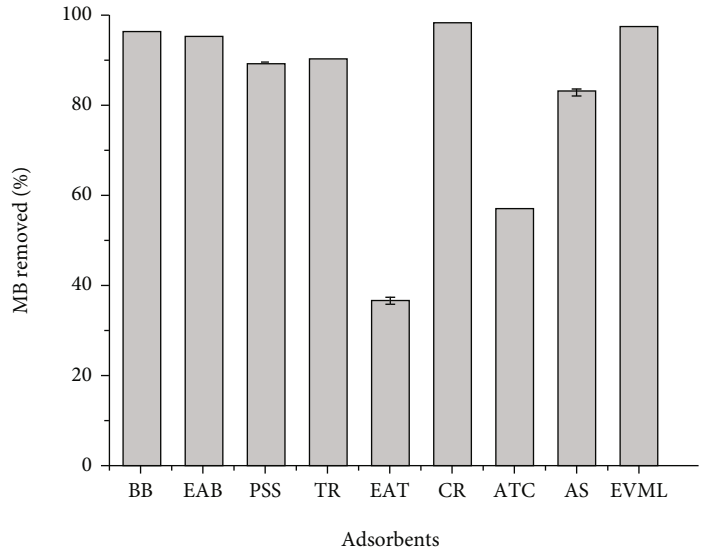

Figure 2: Adsorbents screening test for MB adsorption: initial concentration of MB 10 mg/L, adsorbent dose 2.5 g/L, pH 5.7, agitation time 24 h, shaking speed 200 rpm, and temperature 25 ± 1°C).

in theory, proposing chemisorption as the main MB removal mechanism [27]. The initial MB removal rates (V_0, mg/g min) were computed using the formula $V_0 = k_2 q_{e^2}$, and the *MB* adsorption rate of BB (512 mg/g min) was about 42 times faster than that of EVML (12 mg/g min). This can be due to the variation in the interaction of MB to the active functional group present in BB and EVML. The slope of the curves for both adsorbents is very sharp at the initial stage indicates fast adsorption process with high capacity, which is vital for real uses of the adsorbents to treat dye-contaminated water.

The Weber and Morris model was used to identify the rate-determining step in the MB adsorption process [29] (Eq. (5)). The adsorption process of a certain adsorbate

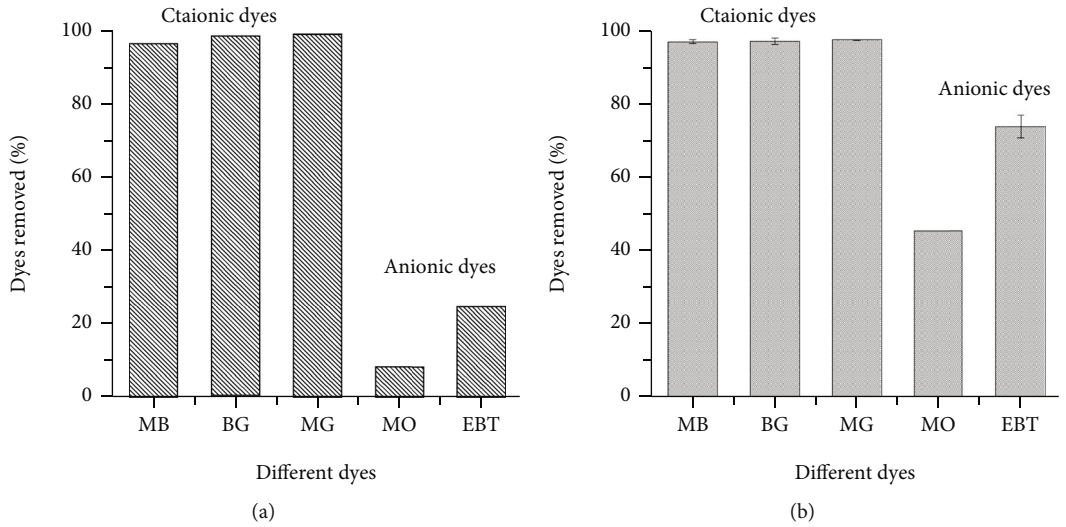

Figure 3: Adsorption performance of BB (a) and EVML (b) for different cationic and anionic dyes (conditions: initial concentration of the dyes 10 mg/L, adsorbent dose 2.5 g/L, agitation time 24 h, shaking speed 200 rpm, and temperature 25 ± 1°C).

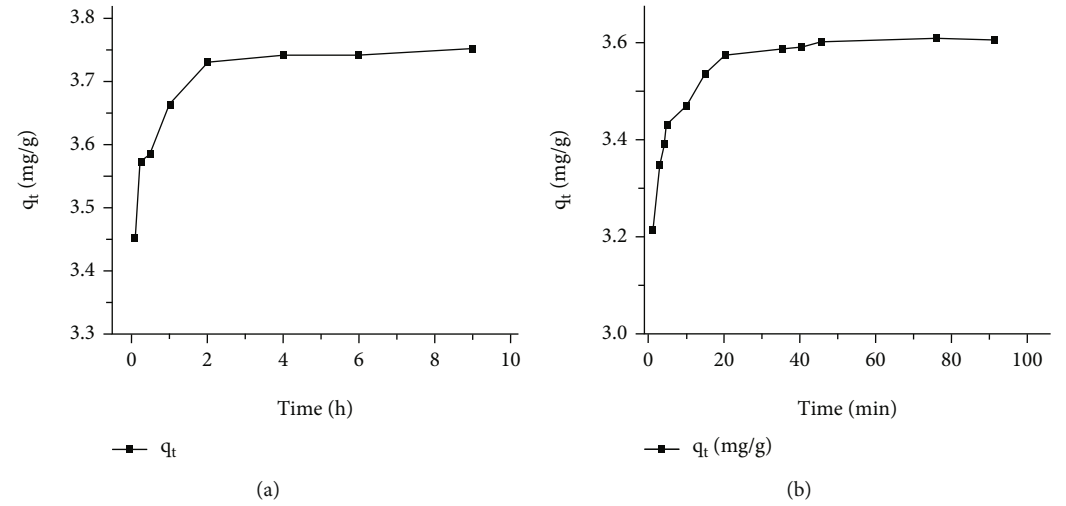

Figure 4: Effect of agitation time on MB removal (a) BB and (b) EVML (conditions: initial concentration (10 mg/L), adsorbent dose (2.5 g/L), shaking speed 200 rpm, and temperature 25 ± 1°C).

usually proceeds through four steps, and these are bulk diffusion, film diffusion, intraparticle or pore diffusion, and adsorption of adsorbate on the adsorbent surface [30]. However, film and/or intraparticle diffusion are usually determine the overall rate of the adsorption process [22, 27]. Figures 6(a) and 6(b) demonstrate the intraparticle diffusion phenomena for the adsorption of MB onto BB and EVML. It is clearly shown that the curves are linear and do not pass through the origin, demonstrating that intraparticle diffusion was not the only rate-determining step. That is, MB adsorption occurs through the engagement of more than one step of the aforementioned four adsorption steps. The obtained results match with previous research findings on adsorption of MB onto various biomasses such as biowaste Papaya stem [27] and chemically modified Bamboo [31].

3.5. Effect of pH. Adsorption processes is significantly affected by pH, since it determine whether an adsorbate is in anionic, neutral, or cationic form and also the surface charge of adsorbents [7]. Increasing the initial pH of MB solution from 2 to 9 for the case of both adsorbents, MB removal efficiency increases from 46% to 97% for BB and from 60% to 97% for EVML (Figures 7(a) and 7(b)). The only exception is pH 3, where 87% and 91% of MB were removed by BB and EVML, respectively. The smaller MB adsorption below pH 3 may be due to the amino and carboxylic acid functional groups being largely protonated, thus resulting in greater electrostatic repulsion for the cationic MB dye [31]. The high MB adsorption onto the adsorbents was observed when the initial pH increases from 4 to 9. The observations were in accordance with earlier findings

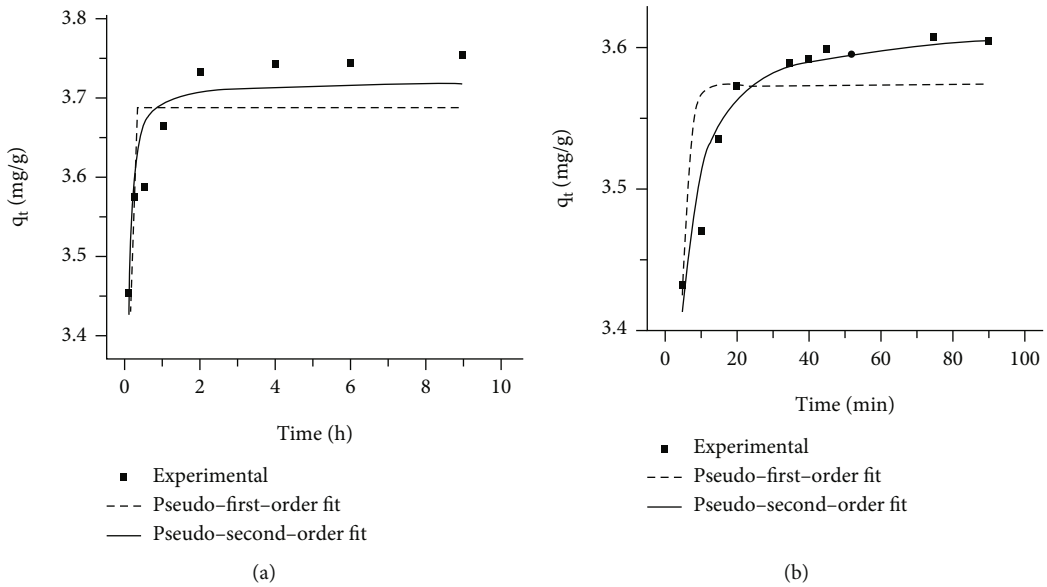

Figure 5: The kinetic models represented by PFO and PSO for (a) BB and (b) EVML.

Table 2: PFO and PSO model parameters for MB adsorption onto BB and EVML.

Parameter	BB		EVML	
	PFO	PSO	PFO	PSO
C_o (mg/L)	10	10	10	10
$q_{e,\exp}$ (mg/g)	3.744	3.744	3.607	3.607
$q_{e,\text{cal}}$ (mg/g)	3.686	3.720	3.573	3.616
k_1 (min^{-1})	33.057	—	0.635	—
k_2 (g/(mg.min))	—	36.995	—	0.926
V_0 (mg/(g.min))	—	511.95	—	12.11
R^2	0.56904	0.83729	0.56676	0.92953
χ^2	6.02×10^{-3}	2.29×10^{-3}	2.02×10^{-3}	3.29×10^{-4}

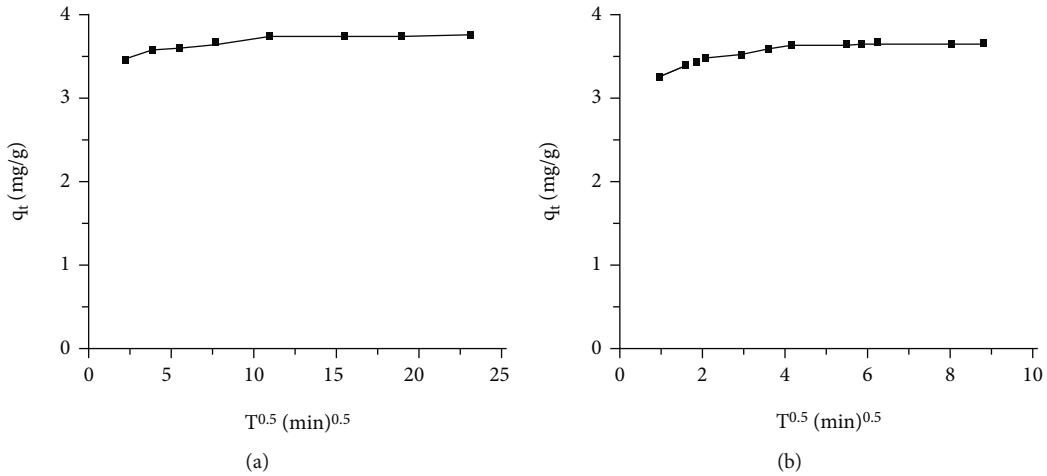

Figure 6: Intraparticle diffusion model plot for the (a) BB and (b) EVML.

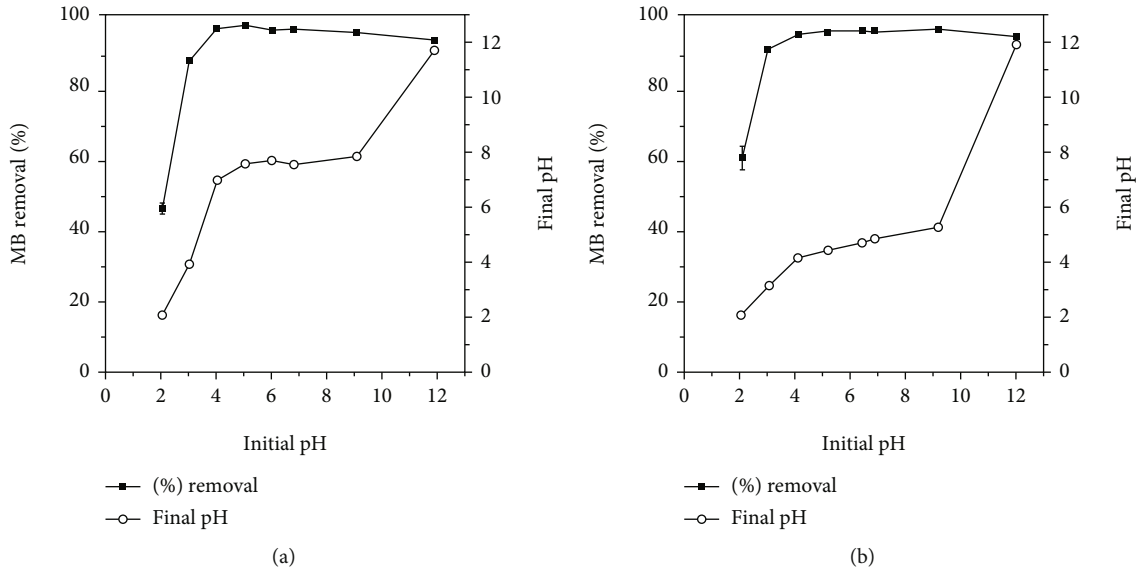

Figure 7: Effect of solution pH on the adsorption of MB onto (a) BB and (b) EVML (conditions: initial concentration 10 mg/L MB, adsorbent dose 2.5 g/L, shaking speed 200 rpm, and temperature 25 ± 1°C).

on MB removal using chemically modified bamboo [31], spent tea leaves [6], and chemically treated agricultural waste [7]. This is interesting in real applications because it avoids the possibility of pH adjustment using an acid and/or a base that may cause secondary pollution. Therefore, the natural pH of MB solution (pH = 5.07) was considered as an ideal pH and used it in further optimization procedures. The high MB removal by both adsorbents in a wide pH range, above and below their pHpzc, suggests the involvement of several interactions like complexation, electrostatic force, and the dipole of the adsorbent surface-polar (cation of the dye) interaction [6].

3.6. Change in Initial MB Concentration. The impact of initial concentration in the adsorption process was assessed by varying the MB concentrations in the range of 10 mg/L to 165 mg/L for BB and 10 mg/L to 105 mg/L for EVML. The obtained results are illustrated in Figures 8(a) and 8(b). As the initial concentration of MB changed from10 mg/L to 165 mg/L, the adsorption capacity of BB improved from 3.68 to 49.11 mg/g, whereas the adsorption capacity of EVML raised from 3.69 to 31.48 mg/g along with an increase in MB concentration from 10 mg/L to 105 mg/L. On the other hand, the percent of MB removal decreased for both adsorbents as the initial concentrations of MB increased. At a lower initial concentration of MB, a few of the adsorbent molecules occupy the adsorbent's surface; therefore, the percent of adsorbate removal is high. However, an increase in the initial MB concentration resulted in coverage of the adsorbent surface by MB molecules, causing in a decline in MB adsorption. This is a common phenomenon in the adsorption process and revealed in results of previous studies on removal of MB by acid-treated banana peel [32], chemically activated Palm fibers [24], and *Parthenium hysterophorus* (an agricultural waste) [7].

3.7. Isotherm. The adoption capacity of an adsorbent usually predicted from isotherm study. Thus, nonlinear Langmuir and Freundlich isothermal equations (Eqs. (6) and (7)) were employed to the experimental MB adsorption data analysis at equilibrium conditions. The plots are shown in Figures 9(a) and 9(b). Table 3 provides the obtained isotherm parameters. The isotherm model that better describes the MB adsorption process was identified by comparing the obtained correlation coefficients (R^2) and chi-square (χ^2) values. The experimental data of MB adsorption onto both adsorbents suited to the Langmuir isotherm, indicating a monolayer adsorption of MB on the surface of the adsorbents [33]. The maximum MB adsorption capacity was 63.2 mg/g and 35.5 mg/g for BB and EVML, respectively. The separation factor (R_L), calculated by the formula $R_L = 1/(1 + bC_0)$, is used to anticipate the feature of the adsorption procedure [17]. The adsorption process is irreversible if $R_L = 0$, favorable if $0 < R_L < 1$, linear if $R_L = 1$, and unfavorable if $R_L > 1$. In this case, the calculated R_L values are between 0 and 1 (Table 3), demonstrating the favorable nature of the adsorption process.

MB is among the toxic cationic basic dyes that are widely used in different industries that requires effective treatment. The effectiveness of BB and EVML adsorbents was compared to some natural and modified adsorbents (Table 4). In general, the maximum adsorption capacity of MB onto the BB and EVML adsorbents was comparable to that of several other natural adsorbents. However, compared with some activated adsorbents such as palm stem and H_2SO_4 activated banana peel, the adsorption capacity of BB and EVML adsorbents was lower. Besides the relatively good adsorption capacities of the biowaste materials, they have also advantages from the perspective of waste reuse to be economically and environmentally safe. The possibility to reuse the adsorbents is an additional asset for these adsorbents.

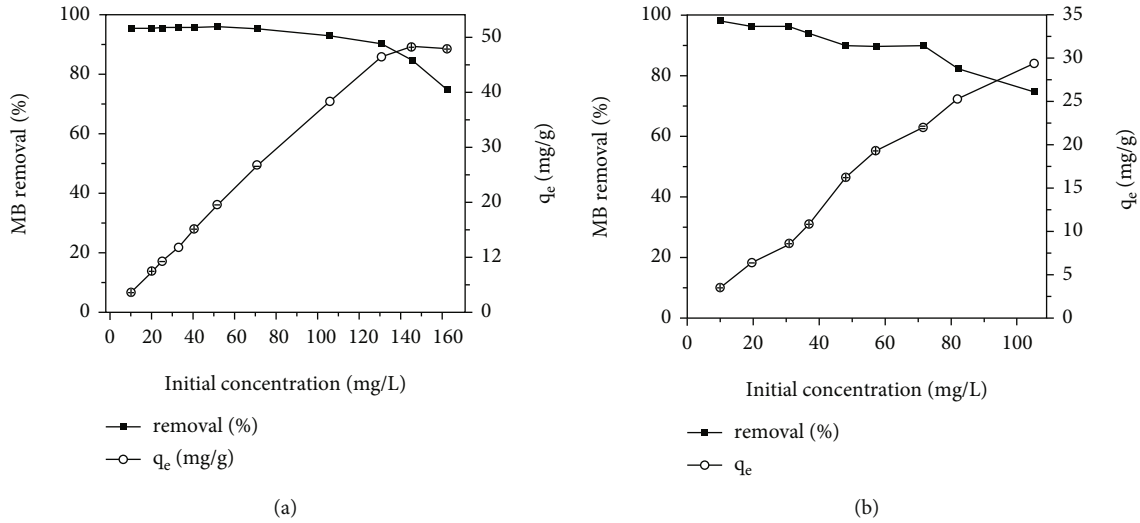

Figure 8: Initial MB concentration variation (a) BB and (b) EVML(conditions: adsorbent dose 2.5 g/L, shaking speed 200 rpm, and temperature 25 ± 1°C).

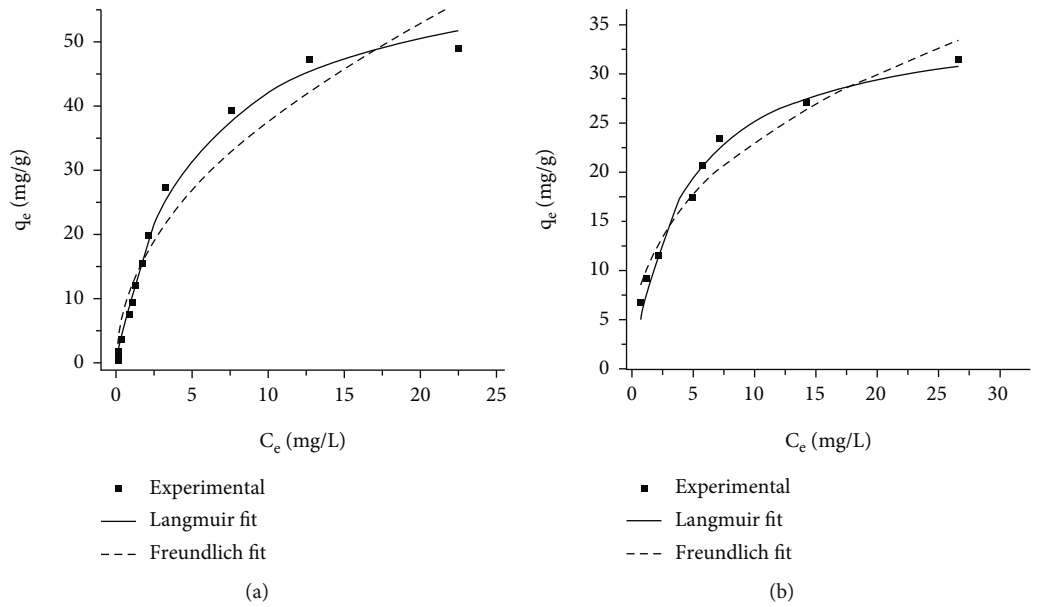

Figure 9: Plot of isotherm models: (a) BB and (b) EVML.

3.8. Adsorption Cycles. The reuse of adsorbents is very vital in producing cost-effective and safe adsorbents. 0.1 M NaOH and 0.1 M HCl solutions were employed in the desorption study. However, the obtained desorption efficiency was not satisfactory. Therefore, the reuse of the adsorbents was assessed without desorption through successive adsorption cycles. The reusability of BB and EVML is presented in Figure 10. The MB removal efficiency of both BB and EVML was not significantly reduced until the 5th cycle. This indicated that the biowaste materials (BB and EVML) were efficient for MB adsorption from contaminated water. The reusability of biowaste materials and their natural accessibility at a very low price makes this method further attractive.

3.9. Feasibility Insights

3.9.1. Economic Feasibility. The cost of water treatment is the most important criterion for an adsorbent or treatment method employed. In adsorption technologies, adsorbent cost-effectiveness is the key constraint that must be considered during adsorbents selection. The cost of an adsorbent can be affected by several factors including its local availability, type of processes required, treatment conditions, recyclability or reusability options, and a lifetime of the adsorbent [41, 42]. The adsorption capacity has also an impact on the cost of the adsorbent material. The techniques to enhance the applicability of the adsorbent material that has a relation

Table 3: Important parameters derived from Langmuir and Freundlich model fittings.

Isotherm	Parameters	BB	EVML
Langmuir	q_{max} (mg/g)	63.23	35.52
	b (L/mg)	0.1978	0.2438
	R_L	0.00123 – 0.0202	0.00232-0.0252
	R^2	0.98973	0.98029
	χ^2	3.43227	1.79086
Freundlich	K_F ($(mg^{1-1/n}L^{1/n})/g$)	11.998	9.784
	N	2.018	2.677
	R^2	0.9311	0.9579
	χ^2	23.0444	3.82589

Table 4: The maximum adsorption capacity of some adsorbents for MB adsorption.

Adsorbents	pH	Q_{max} (mg/g)	Equilibrium time (h)	Dose (g/L)	Reference
Wheat shell	5-9	16.6	1	10	[34]
Rice husk	—	40.6	0.67	4	[35]
Activated carbon from palm stem	6	110.8	0.3	1.25	[24]
Date palm leaf powder	6.5	43.1	2.67	10	[36]
Neem leaf powder	5-8	8.8	—	—	[37]
Rice husk	5-7	21.9	24	6	[38]
Rice husk ash	5-7	12.8	24	6	[38]
H_2SO_4 activated banana peel	10	250.0	24	0.8	[32]
Sugarcane bagasse	—	9.4	24	2.0	[39]
Tea waste	8	113.1	24	4.0	[40]
BB	5.07	63.2	4	2.5	Present study
EVML	5.66	35.5	1	2.5	Present study

to the cost including regeneration, reusability; and high capacity of the adsorbents should be taken into account in cost-benefit analysis. Table 5 presents cost estimates for some reported adsorbents for MB removal. Most often, the cost estimation is rarely reported in literature briefing simply "low-cost" that might be obtained by considering the cost of the raw materials. However, all considerations of local availability, processing, transportation costs, recyclability, and a lifetime of adsorbent material are found vital [43]. The costs of BB and EVML are quite good in comparison with other adsorbents (Table 5). For instance, it was found to have only processing costs as both adsorbents are sourced from byproducts/wastes. Comparison of the costs of the adsorbents is not straightforward due to variations in adsorption capacity, regional processing fees, experimental level, and large-scale conditions. Furthermore, material costs, energy costs, capital costs, and other miscellaneous detail costs are required to be evaluated for large-scale applications. Hence, locally available and low-cost materials as is the case in this study predicted from lab-scale experiments have paramount importance as an alternative adsorbent. In general, the reusability of both adsorbents, BB and EVML, can work for more than five cycles in the adsorption process, local availability, and abundance. Enset and barley are widely cultivated in Ethiopia [44] indicating the promising availability of BB and EVML and their feasibility for the targeted application. Both BB and EVML adsorbents could have a potential to substitute commercially available activated carbon at a lower cost. Industrial-scale treatments of dye wastewater using bio-adsorbents were considered promising at large due to availability and cost benefits [43].

3.9.2. Technical Feasibility and Environmental Safety. Most often, carbonization, physical activation, and chemical activation are commonly employed in adsorbent preparation processes that incur costs to a certain extent. The leaching from the adsorbents could be a limiting factor in water treatment applications; however, the adsorbents, BB, and EVML are part of edible crops that are expected to be less likely to leach toxic chemicals. This is because enset and barley are among the staple foods of Ethiopians, and the level of contaminants including heavy metal contents is well studied [44]. Processing and putting into batches and column set up of these adsorbents are easier and adaptable due to the traditional use of these materials in water storage clay pot preparations.

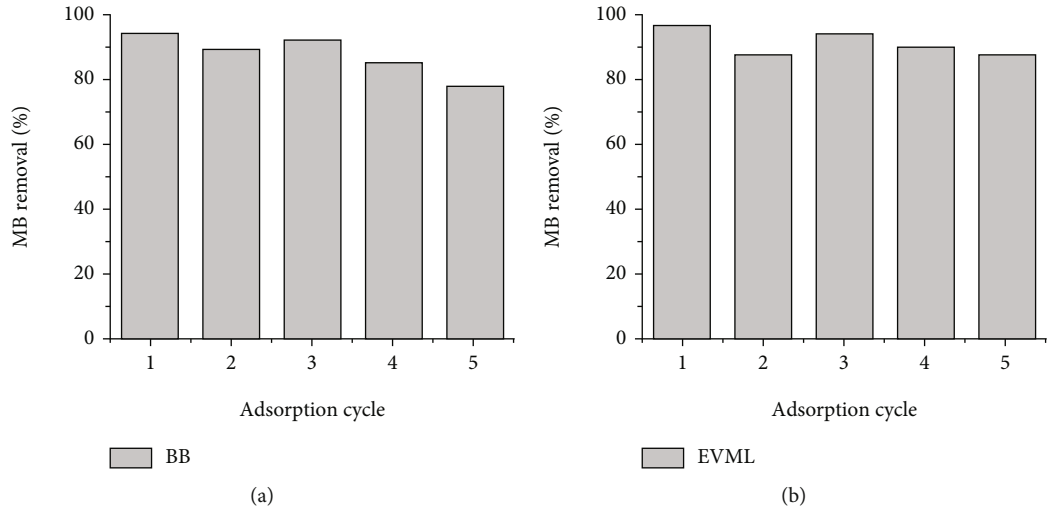

Figure 10: Adsorption cycle of (a) BB and (b) EVML for MB removal.

Table 5: Comparative presentation of costs of adsorbents.

Adsorbents	Cost USD/kg	Reference
Activated carbon from nutshells	2.15	[45]
Virgin carbon	0.86-2.95	[46]
Reactivated carbon	0.43-0.70	[47]
Alumina	0.03	[48]
Sludge-based adsorbents	0.1-0.2	[41]
Clay minerals	0.04-0.12	[49]
Zeolite	0.14-0.8	[48, 50]
Diatomite	0.011-1.10	[48]
BB	<0.012 (processing cost only)	Current study
EVML	<0.02 (processing cost only)	Current study

3.9.3. Accessibility. Accessibility of the adsorbent material in adsorption technology could contribute to cost savings. Hence, understanding the local availability and abundance of materials BB and EVML is vital. Enset is one of the staple foods of Ethiopia consumed by more than 20 million people due to its high starch content [51], from where EVML is produced. The dry matter content of lamina and midribs of leaves of enset is estimated to be 15–17% [52]. It is a multipurpose tree that has been found abundantly, especially in South Ethiopia. Enset grows in East and Southern Africa, and the genus extends across Asia to China; however, it is domesticated only in the Ethiopian [53]. And Ethiopia is the second-largest barley producer in Africa [54]. Barley bran is a byproduct of barley processes, and it is brittle and shatters of barley.

4. Conclusion

In this paper, several biowaste materials were screened for MB removal from an aqueous solution, which is in line with the concept of waste reuse. Among them, BB and EVML were selected based on their performances. The obtained results show that the MB dye was adsorbed between pH 4 and 9. The maximum predicted adsorption capacities were found to be 63.2 mg/g for BB and 35.5 mg/g for EVML as obtained from the well-fitting Langmuir isotherm model. Results of the kinetic studies suggested that the adsorption phenomena can be explained by using PSO kinetics, suggesting chemisorption as the main adsorption mechanism. The biowaste materials (BB and EVML) can be reused in multiple adsorption cycles (without desorption), being MB removal efficiencies above 80% until the 5^{th} cycle. Therefore, it can be concluded that the use of these biowaste materials has promising feasibility. Further studies should focus on the performance and scalability of using adsorbents on real wastewaters in a column study.

Data Availability

The datasets used and/or analyzed during the current study are available from the corresponding author on reasonable request.

Additional Points

Highlights. Biowaste materials were used to clean up dye-contaminated water. Chemisorption was a possible mechanism of MB dye adsorption. Biowaste materials were effective in removing cationic dyes rather than anionic dyes. The adsorbents perform very well in a wide pH range (4–9).

Conflicts of Interest

The authors declare that they have no conflicts of interest.

Authors' Contributions

TG and FM conceived the idea of this study, supervised the experimental work, and edited the manuscript. DM performed the experiments and process results in graphs and tables. AD drafted the manuscript.

Acknowledgments

We declare that this work was carried out by the support of Jimma University MSc Students' Research Fund.

References

[1] A. Ameta, R. Ameta, and M. Ahuja, "Photocatalytic degradation of methylene blue over ferric tungstate," *Scientific Reviews and Chemical Communications*, vol. 3, pp. 172–180, 2013.

[2] H. N. J. Hoong and N. Ismail, "Removal of Dye in Wastewater by Adsorption-Coagulation Combined System withHibiscus sabdariffaas the Coagulant," *MATEC Web of Conferences*, vol. 152, article 01008, 2018.

[3] F. Wei, M. J. Shahid, G. S. H. Alnusairi et al., "Implementation of floating treatment wetlands for textile wastewater management: a review," *Sustain*, vol. 12, no. 14, pp. 5801–5829, 2020.

[4] R. Chikri, N. Elhadiri, M. Benchanaa, and Y. El, "Efficiency of Sawdust as Low-Cost Adsorbent for Dyes Removal," *Journal of Chemistry*, vol. 2020, 17 pages, 2020.

[5] R. Kant, "Textile dyeing industry an environmental hazard," *Natural Science*, vol. 4, no. 1, pp. 22–26, 2012.

[6] B. H. Hameed, "Spent tea leaves: a new non-conventional and low-cost adsorbent for removal of basic dye from aqueous solutions," *Journal of Hazardous Materials*, vol. 161, no. 2-3, pp. 753–759, 2009.

[7] H. Lata, V. K. Garg, and R. K. Gupta, "Removal of a basic dye from aqueous solution by adsorption using Parthenium hysterophorus: an agricultural waste," *Dyes and Pigments*, vol. 74, no. 3, pp. 653–658, 2007.

[8] K. A. Adegoke and O. Solomon, "Dye sequestration using agricultural wastes as adsorbents," *Water Resources and Industry*, vol. 12, pp. 8–24, 2015.

[9] A. U. Khan, M. U. Rehman, M. Zahoor, A. B. Shah, and I. Zekker, "Biodegradation of brown 706 dye by bacterial strain pseudomonas aeruginosa," *Water*, vol. 13, no. 21, p. 2959, 2021.

[10] S. Shakoor and A. Nasar, "Removal of methylene blue dye from artificially contaminated water using citrus limetta peel waste as a very low cost adsorbent," *Journal of the Taiwan Institute of Chemical Engineers*, vol. 66, pp. 154–163, 2016.

[11] K. S. Bharathi and S. T. Ramesh, "Removal of dyes using agricultural waste as low-cost adsorbents : a review," *Applied Water Science*, vol. 3, pp. 773–790, 2013.

[12] M. Asgher and H. N. Bhatti, "Evaluation of thermodynamics and effect of chemical treatments on sorption potential of _Citrus_ waste biomass for removal of anionic dyes from aqueous solutions," *Ecological Engineering*, vol. 38, no. 1, pp. 79–85, 2012.

[13] J. O. Quansah, T. Hlaing, F. N. Lyonga et al., "Nascent rice husk as an adsorbent for removing cationic dyes from textile wastewater," *Applied Sciences*, vol. 10, no. 10, p. 3437, 2020.

[14] J. Fito, S. Abrham, and K. Angassa, "Adsorption of methylene blue from textile industrial wastewater onto activated carbon of Parthenium hysterophorus," *International Journal of Environmental Research*, vol. 14, no. 5, pp. 501–511, 2020.

[15] J. O. Amode, J. H. Santos, A. H. Mirza, and C. C. Mei, "Adsorption of methylene blue from aqueous solution using untreated and treated (Metroxylon spp.) waste adsorbent: equilibrium and kinetics studies," *International Journal of Industrial Chemistry*, vol. 7, no. 3, pp. 333–345, 2016.

[16] A. Kebede, K. Kedir, F. Melak, and T. G. Asere, "Removal of Cr(VI) from aqueous solutions using biowastes: Tella residue and pea *(Pisum sativum)* seed shell," *Scientific World Journal*, vol. 2022, article 7554133, 2022.

[17] T. G. Asere, J. De Clercq, K. Verbeken et al., "Uptake of arsenate by aluminum (hydr)oxide coated red scoria and pumice," *Applied Geochemistry*, vol. 78, pp. 83–95, 2017.

[18] M. N. Sepehr, M. Zarrabi, H. Kazemian, A. Amrane, K. Yaghmaian, and H. R. Ghaffari, "Removal of hardness agents, calcium and magnesium, by natural and alkaline modified pumice stones in single and binary systems," *Applied Surface Science*, vol. 274, pp. 295–305, 2013.

[19] T. Adane, D. Haile, A. Dessie, Y. Abebe, and H. Dagne, "Response surface methodology as a statistical tool for optimization of removal of chromium (VI) from aqueous solution by Teff (Eragrostis teff) husk activated carbon," *Applied Water Science*, vol. 10, no. 1, 2020.

[20] S. Maulina and M. Iriansyah, "Characteristics of activated carbon resulted from pyrolysis of the oil palm fronds powder," in *IOP Conference Series: Materials science and Engineering*, Sumatera Utara, Indonesia, 2018.

[21] N. Y. Al-awwal and U. L. Ali, "Proximate analyses of different samples of egg shells obtained from Sokoto market in Nigeria," *International Journal of Science and Research*, vol. 4, pp. 564–566, 2015.

[22] T. G. Asere, S. Mincke, K. Folens et al., "Dialdehyde carboxymethyl cellulose cross-linked chitosan for the recovery of palladium and platinum from aqueous solution," *Reactive and Functional Polymers*, vol. 141, pp. 145–154, 2019.

[23] M. K. Uddin and A. Nasar, "Walnut shell powder as a low-cost adsorbent for methylene blue dye: isotherm, kinetics, thermodynamic, desorption and response surface methodology examinations," *Scientific Reports*, vol. 10, no. 1, article 7983, 2020.

[24] L. S. Maia, A. I. C. da Silva, E. S. Carneiro, F. M. Monticelli, F. R. Pinhati, and D. R. Mulinari, "Activated carbon from palm fibres used as an adsorbent for methylene blue removal," *Journal of Polymers and the Environment*, vol. 29, no. 4, pp. 1162–1175, 2021.

[25] S. Yasar and R. Tosun, "Predicting chemical, enzymatic and nutritional properties of fermented barley (Hordeum vulgare L.) by second derivate spectra analysis from attenuated total

reflectance-Fourier transform infrared data and its nutritional value in Japanese quails," *Archives of Animal Nutrition*, vol. 72, no. 5, pp. 407–423, 2018.

[26] J. Zhao, W. Xiuwen, J. Hu, Q. Liu, D. Shen, and R. Xiao, "Thermal degradation of softwood lignin and hardwood lignin by TG-FTIR and Py-GC/MS," *Polymer Degradation and Stability*, vol. 108, pp. 133–138, 2014.

[27] R. R. Krishni, K. Y. Foo, and B. H. Hameed, "Adsorption of cationic dye using a low-cost biowaste adsorbent: equilibrium, kinetic, and thermodynamic study," *Desalination and Water Treatment*, vol. 52, no. 31-33, pp. 6088–6095, 2014.

[28] S. A. Ali, S. A. Mubarak, I. Y. Yaagoob, Z. Arshad, and M. A. J. Mazumder, "A sorbent containing pH-responsive chelating residues of aspartic and maleic acids for mitigation of toxic metal ions, cationic, and anionic dyes," *RSC Advances*, vol. 12, no. 10, pp. 5938–5952, 2022.

[29] S. P. S. Markandeya and G. C. Kisku, "Linear and non-linear kinetic modeling for adsorption of disperse dye in batch process," *Research Journal of Environmental Toxicology*, vol. 9, no. 6, pp. 320–331, 2015.

[30] S. Nethaji, A. Sivasamy, and A. B. Mandal, "Adsorption isotherms, kinetics and mechanism for the adsorption of cationic and anionic dyes onto carbonaceous particles prepared from Juglans regia shell biomass," *International journal of Environmental Science and Technology*, vol. 10, no. 2, pp. 231–242, 2013.

[31] J. Z. Guo, B. Li, L. Liu, and K. Lv, "Removal of methylene blue from aqueous solutions by chemically modified bamboo," *Chemosphere*, vol. 111, pp. 225–231, 2014.

[32] A. H. Jawad, R. A. Rashid, M. A. M. Ishak, and K. Ismail, "Adsorptive removal of methylene blue by chemically treated cellulosic waste banana (Musa sapientum) peels," *Journal of Taibah University for Science*, vol. 12, no. 6, pp. 809–819, 2018.

[33] N. R. P. A. Pargami and M. S. A. N. Emami, "Surfactant-coated tea waste: preparation, characterization and its application for methylene blue adsorption from aqueous solution," *Journal of Environmental & Analytical Toxicology*, vol. 5, no. 5, 2015.

[34] Y. Bulut and H. Aydin, "A kinetics and thermodynamics study of methylene blue adsorption on wheat shells," *Desalination*, vol. 194, no. 1-3, pp. 259–267, 2006.

[35] V. Vadivelan and K. Vasanth Kumar, "Equilibrium, kinetics, mechanism, and process design for the sorption of methylene blue onto rice husk," *Journal of Colloid and Interface Science*, vol. 286, no. 1, pp. 90–100, 2005.

[36] M. Gouamid, M. R. Ouahrani, and M. B. Bensaci, "Adsorption equilibrium, kinetics and thermodynamics of methylene blue from aqueous solutions using date palm leaves," *Energy Procedia*, vol. 36, pp. 898–907, 2013.

[37] M. A. Mohammed, A. Shitu, and A. Ibrahim, "Removal of Methylene Blue Using Low Cost Adsorbent: A Review," *Research Journal of Chemical Sciences*, vol. 4, pp. 91–102, 2014.

[38] D. Phihusut and M. Chantharat, "Removal of methylene blue using agricultural waste: a case study of rice husk and rice husk ash from Chaipattana rice mill demonstration center," *Environment and Natural Resources Journal*, vol. 15, pp. 30–38, 2017.

[39] T. C. Andrade Siqueira, I. Zanette da Silva, A. J. Rubio et al., "Sugarcane bagasse as an efficient biosorbent for methylene blue removal: kinetics, isotherms and thermodynamics," *International Journal of Environmental Research and Public Health*, vol. 17, no. 2, 2020.

[40] D. S. Malik, C. K. Jain, A. K. Yadav, R. Kothari, and V. V. Pathak, "Removal of methylene blue dye in aqueous solution by agricultural waste," *International Research Journal of Innovations in Engineering and Technology*, vol. 3, no. 7, pp. 1–7, 2016.

[41] P. Devi and A. K. Saroha, "Utilization of sludge based adsorbents for the removal of various pollutants: a review," *Science of the Total Environment*, vol. 578, pp. 16–33, 2017.

[42] S. A. Hamid, M. Shahadat, and S. Ismail, "Development of cost effective bentonite adsorbent coating for the removal of organic pollutant," *Applied Clay Science*, vol. 149, pp. 79–86, 2017.

[43] W. Li, B. Mu, and Y. Yang, "Feasibility of industrial-scale treatment of dye wastewater via bio-adsorption technology," *Bioresource Technology*, vol. 277, pp. 157–170, 2019.

[44] B. Teressa and A. Alemayehu, "Metallic nutrients in enset (Ensete Ventricosum) corm and soil sample from some west Shoa zone, Oromia regional State, Ethiopia," *International Journal of Agricultural Science and Food Technology*, vol. 7, pp. 073–080, 2021.

[45] M. León, J. Silva, S. Carrasco, and N. Barrientos, "Design, cost estimation and sensitivity analysis for a production process of activated carbon from waste nutshells by physical activation," *PRO*, vol. 8, no. 8, p. 945, 2020.

[46] N. Passarella, *(Calgon carbon corporation) to Amanda Baynham*, RTI International, 2018.

[47] Ken Kikta, "Carbtrol Corporation, Bridgeport C to AB (RTI, International, Research Triangle Park N)," *Carbon Adsorber*, vol. 18, 2018.

[48] U.S. Geological Survey, *Mineral commodity summaries 2021*, U.S. Geological Survey, 2021.

[49] G. McMahon, S. P. Benjamin, K. Clarke et al., "Geography for a changing world: A science strategy for the geographic research of the U.S. Geological Survey, 2005-2015," *Circular*, vol. 1281, pp. 1–74, 2005.

[50] G. Xu, X. Yang, and L. Spinosa, "Development of sludge-based adsorbents: preparation, characterization, utilization and its feasibility assessment," *Journal of Environmental Management*, vol. 151, pp. 221–232, 2015.

[51] J. S. Borrell, M. Goodwin, G. Blomme et al., "Enset-Based Agricultural Systems in Ethiopia: A Systematic Review of Production Trends, Agronomy, Processing and the Wider Food Security Applications of a Neglected Banana Relative," *Plants People Planet*, vol. 2, no. 3, pp. 212–228, 2020.

[52] H. Berhanu, Z. Kiflie, I. Miranda et al., "Characterization of crop residues from false banana /ensete ventricosum/ in Ethiopia in view of a full-resource valorization," *PLoS One*, vol. 13, no. 7, p. e0199422, 2018.

[53] J. S. Borrell, M. K. Biswas, M. Goodwin et al., "Enset in Ethiopia: A poorly characterized but resilient starch staple," *Annals of Botany*, vol. 123, no. 5, pp. 747–766, 2019.

[54] D. Tadesse and B. Derso, "The status and constraints of food barley production in the North Gondar highlands, North Western Ethiopia," *Agriculture & Food Security*, vol. 8, no. 1, 2019.